

# MUSE: Illustrating Textual Attributes by Portrait Generation

Xiaodan Hu<sup>1</sup>, Pengfei Yu<sup>1</sup>, Kevin Knight<sup>2</sup>, Heng Ji<sup>1</sup>  
Bo Li<sup>1</sup>, Honghui Shi<sup>1</sup>

<sup>1</sup>University of Illinois at Urbana-Champaign

<sup>2</sup>DiDi Labs

{xiaodan8, pengfei4, hengji, lbo, hshi10}@illinois.edu,  
kevinknight@didiglobal.com,

## Abstract

We propose a novel approach, MUSE, to illustrate textual attributes visually via portrait generation. MUSE takes a set of attributes written in text, in addition to facial features extracted from a photo of the subject as input. We propose 11 attribute types to represent inspirations from a subject’s profile, emotion, story, and environment. We propose a novel stacked neural network architecture by extending an image-to-image generative model to accept textual attributes. Experiments show that our approach significantly outperforms several state-of-the-art methods without using textual attributes, with Inception Score score increased by 6% and Fréchet Inception Distance (FID) score decreased by 11%, respectively. We also propose a new attribute reconstruction metric to evaluate whether the generated portraits preserve the subject’s attributes. Experiments show that our approach can accurately illustrate 78% textual attributes, which also help MUSE capture the subject in a more creative and expressive way.<sup>1</sup>

## 1. Introduction

The current popular language models learned from large-scale data sets still cannot well represent abstract attributes. Table 1 shows the top 10 nearest words of abstract attributes acquired using a typical language model (LM) learned from large-scale textual data [1]. We can see a textual LM often fails to represent these abstract attributes. In contrast, human can illustrate abstract concepts at early age visually. For example, Figure 1 shows various children’s drawings about the concept “family”, by using sun and smiling faces to represent happiness, and height to distinguish parents and children.

We aim to teach computer to automatically illustrate tex-

<sup>1</sup>We will make all of the data sets, resources and programs related to this new benchmark publicly available.



Figure 1. Children’s illustrations about “family”.

tual attributes by generating portraits. Portrait is a special genre in painting, where the goal is to present not only the outward appearance of a specific human subject, but also their inner significance inspired by admiration or affection for the subject. A good portrait needs to be realistic, and thus it’s important to take a photo of the subject as input. Some recent attempts [2, 3, 4, 5] try to automate the conversion from photo to portrait. Most of these methods are only based on visual style transfer [2, 3, 6]. However, art works reflect not only the artist’s hard work and dexterous technique but also often carry their personal emotions and memories on the subjects, due to the intimate relationship between the artist and the subject, either bound together before or during the painting. As Aristotle stated, “The aim of Art is to present not the outward appearance of things, but their inner significance; for this, not the external manner and detail, constitutes true reality.” [7]. From a good portrait, we can often reveal the story of the subject’s life, such as occupation, hobby, personality, mood, or a special occasion which may even involve the artist, from a certain facial expression, hairstyle, or the artist’s clever use of colors and lines.

We represent a story (i.e. the inspirations) of the sub-

Abstract Attribute	Top 10 Nearest Words
happy	<b>'m</b> ; glad; pleased; <b>really</b> ; <b>always</b> ; <b>everyone</b> ; <b>everybody</b> ; <b>feel</b> ; <b>i</b> ; <b>sure</b>
calm	quiet; <b>jittery</b> ; <b>tense</b> ; peaceful; tranquil; calmed; serene; calming; calmness; relaxed
hot	<b>cool</b> ; hottest; heat; warm; <b>cold</b> ; <b>chili</b> ; <b>dry</b> ; heated; bubbling; hotter
cold	<b>warm</b> ; cool; chill; <b>temperatures</b> ; chilly; <b>dry</b> ; freezing; frigid; <b>weather</b> ; winter
rainy	windy; <b>weather</b> ; <b>monsoon</b> ; rains; humid; chilly; rain; <b>sunny</b> ; <b>winters</b> ; rainfall
sunny	<b>breezy</b> ; <b>windy</b> ; balmy; <b>chilly</b> ; <b>sunshine</b> ; <b>cloudy</b> ; <b>rainy</b> ; warm; <b>skies</b> ; <b>cool</b>
cloudy	overcast; <b>sunny</b> ; <b>skies</b> ; chilly; <b>windy</b> ; <b>breezy</b> ; <b>rainy</b> ; hazy; <b>humid</b> ; foggy
windy	blustery; chilly; <b>rainy</b> ; <b>sunny</b> ; breezy; <b>muggy</b> ; <b>foggy</b> ; <b>humid</b> ; <b>snowy</b> ; <b>balmy</b>
foggy	<b>windy</b> ; <b>rainy</b> ; <b>chilly</b> ; <b>snowy</b> ; fog; dreary; <b>frigid</b> ; <b>drizzly</b> ; hazy; damp
snowy	frigid; icy; <b>windy</b> ; <b>rainy</b> ; wintry; <b>foggy</b> ; chilly; <b>blustery</b> ; <b>mountains</b> ; <b>mountainside</b>

Table 1. Top 10 nearest words of abstract attributes acquired using GloVe [1] language model learned from large-scale textual data. The bold words not semantically similar to the attributes.

Text Attribute	Value Examples	#Values
Age	Child; Young adults; Middle-aged adults; Older adults	4
Clothing	Blazer; Coat and Jacket; Choir & Religious Robe; Dressing Gown; Dress; Shirt; Sweater	14
Facial Expression	Smile; Smirk; Sneer; Glance; Wink; Wrinkle the nose; Long face; Blank expression	14
Gender	Male; Female; Other	3
Hair	Straight hair; Wavy hair; Black hair; Blond hair; Short hair	5
Mood	Calm; Excited; Happy; Angry; Apathetic; Sad	6
Pose & Gesture	Lying; Sitting; Squatting or crouching; Standing; Riding; Shooting; Sleeping; Bowing	9
Setting	In the room; In the hallway; On the street; At the river; In the courtyard or a garden	9
Style	Impressionism; Realism; Classical Art; Modernism; Chinese paintings; Japanese paintings	7
Time	Before 1970; After 1970	2
Weather	Rainy; Stormy; Sunny; Cloudy; Hot; Cold; Windy; Foggy; Snow	9

Table 2. Text Attributes to Represent Portrait Inspirations.

ject with 11 text attributes, as shown in Table 2, including mood, facial expression, gender and hairstyle. We design a new portrait generation framework called *MUSE*, which takes these inspirational textual attributes in addition to face regions as input for portrait generation. We first feed the extracted face from the input photo into the encoder part of a UNet [8], a convolutional network architecture that has show promising results on image generation [9, 10]. Then we directly feed the textual attributes into an attribute encoder. Finally the textual attribute embeddings are integrated with the hidden representation of the input photo as an input to the attribute-based decoder to generate the portrait. Figure 2 illustrates an example where the facial expression and hair style are automatically changed based on a set of attributes expressed in text.

Moreover, existing evaluation metrics such as Inception Score (IS) [11] only check the overlapped visual content between the machine-generated and human-generated portraits. But this is not how human assessors approach and appreciate a painting. We design a novel metric to evaluate how many text attributes human assessors can reconstruct from the system generated portraits. Experiments show that our method outperforms state-of-the-art on all measures, and portrait generation is an effective way to acquire and illustrate textual attributes.

In summary, the main contributions of this paper are as

follows:

- We propose the first inspiration-to-portrait generation framework *MUSE* that takes text description of attributes into account to generate portraits aligned with its background story such as underlying emotions.
- We develop a novel neural network architecture incorporating textual attributes for portrait generation. Rather than using a binary sequence of facial attributes as input, we apply attribute embeddings, which are initialized from portrait data and optimized during training. Instead of preserving the attributes of input photos, we design a novel discriminator to encourage diversity and realism.
- We create a large portrait generation data set containing 3,928 photo-portrait pairs with manually annotated attributes as a new benchmark, along with 51,939 portraits without annotations, and will share the resources with the community for further exploration.
- We propose a novel evaluation metric based on human attribute reconstruction to better assess the quality of generated portraits.

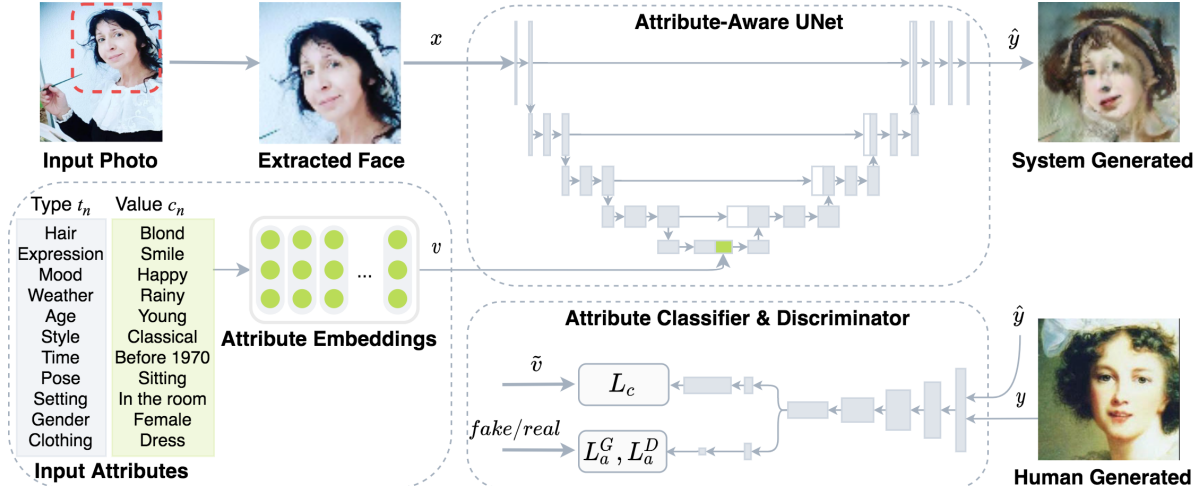


Figure 2. Overview of the model architecture. Given an input photo  $x$  and attribute embeddings  $\mathbf{v}$ , the model can generate the portrait  $\hat{y}$ . The generator  $G$  is an attribute-aware UNet that incorporate attribute embeddings in hidden representation. The discriminator  $D$  is a stack of convolutional layers followed by fully connected layers. By using the adversarial loss function,  $L_a$ , and the attribute classification loss functions,  $L_c$ , the discriminator  $D$  can not only recognize the realism of the generated portrait  $\hat{y}$  but also classify  $\hat{y}$  into different class of each attribute.

## 2. MUSE: Portrait Generation Approach

*MUSE* takes two sources of input to generate portraits: (1) a photo  $x$  of the subject; (2) a set of textual attributes in form of type-value pairs  $\{(t_i, c_i)\}_{i=1}^n$ . *MUSE* contains a generator  $G$  and a corresponding discriminator  $D$  for adversarial training. To demonstrate the importance and effectiveness of textual attributes, we modify a state-of-the-art image generator, UNet [8, 10], to incorporate attribute embeddings  $v$  into generation. The discriminator  $D$  takes the system generated portrait  $\hat{y}$  together with its corresponding human generated portrait  $y$  to evaluate the generator  $G$ . The overall architecture of *MUSE* is depicted in Figure 2.

### 2.1. Attribute Embedding

We propose 11 textual attributes to represent the inspirations, as shown in Table 2. We select these attributes from various online resources including the LitCharts Library, ClarkandMiller.com, and ManyThings.org.

We assign each type-value pair  $(t_i, c_i)$  a unique embedding  $\mathbf{v}_i$ . Given a set of  $n$  attribute type-value pairs  $\{(t_i, c_i)\}_{i=1}^n$  as input, we concatenate embeddings for  $n$  pairs to get the input attribute embedding  $\mathbf{v} = [\mathbf{v}_1; \mathbf{v}_2; \dots; \mathbf{v}_n] \in \mathbb{R}^{nd_w}$ .

The attribute values in Table 2 are correlated. For instance, we find that the clothing under rainy weather is more likely to be blazer or coat. To capture such interdependency between multiple attribute values, we initialize  $\mathbf{v}_i$  by using domain-specific attribute embeddings trained from portrait data, where we use skip-gram methods in Word2Vec [12] and consider attribute values corresponding to the same portrait as a bag of words in one context

window.

### 2.2. Attribute-aware UNet

UNet [8, 10] is a high-quality image-to-image generative model. Given an input photo  $x$ , UNet first encodes  $x$  into a hidden representation  $\mathbf{h} \in \mathbb{R}^{d_h} = G_{enc}(x)$  using multi-layer Convolutional Neural Networks (CNNs), which is further decoded into an output image  $\hat{y} = G_{dec}(\mathbf{h})$  using a stack of transposed convolutional layers.

Our generator  $G$  employs the UNet architecture. The input photo  $x$  is first encoded into the hidden representation  $\mathbf{h}$ . Then we aggregate the hidden representation  $\mathbf{h}$  and attribute embeddings  $\mathbf{v}$  of the expected portrait as

$$\mathbf{h}^a = \sigma(\mathbf{W}_h \mathbf{h} + \mathbf{W}_v \mathbf{v} + \mathbf{b}),$$

where  $\mathbf{W}_h \in \mathbb{R}^{d_h \times d_h}$ ,  $\mathbf{W}_v \in \mathbb{R}^{d_h \times nd_w}$  and  $\mathbf{b} \in \mathbb{R}^{d_h}$  are learnable parameters.  $\sigma$  is an activation function and we use ReLU [13]. We decode the portrait as  $\hat{y} = G_{dec}(\mathbf{h}^a)$ . For simplicity, we use  $G_{enc}^a(x, \mathbf{v})$  to represent  $\mathbf{h}^a$ .

### 2.3. Loss Functions

We apply adversarial training simultaneously for the generator and discriminator ( $G, D$ ) to learn the mapping from the input photos  $X$  and input attribute embeddings  $V$  to the output portraits  $Y$ . Given training samples  $\{(x^{(i)}, \mathbf{v}^{(i)}, y^{(i)})\}_{i=1}^N$  where the input photo  $x^{(i)} \in X$ , input attribute embeddings  $\mathbf{v}^{(i)} \in V$  and the human generated portrait  $y^{(i)} \in Y$ , we denote the data distribution as  $x \sim p_{data(x)}$ ,  $\mathbf{v} \sim p_{attr}$  and  $y \sim p_{data(y)}$ . While  $G$  tries to generate realistic portraits  $\hat{y}$  similar to the portraits  $y$  in  $Y$  domain,  $D$  tries to distinguish between  $\hat{y}$  and  $y$ .

We compute the adversarial loss following GAN [14], with input photo  $x$ , attribute embeddings  $\mathbf{v}$ , and  $y$  as corresponding human generated portraits rescaled to the same size as the outputs of  $G$ . Specifically, the adversarial losses of the generator  $G_i$  and discriminator  $D$  are formulated as follows:

$$\mathcal{L}_a^G = -\mathbb{E}_{x \sim p_{\text{data}(x)}, \mathbf{v} \sim p_{\text{attr}}} \log D(G_{\text{dec}}(G_{\text{enc}}^a(x, \mathbf{v}))), \quad (1)$$

$$\mathcal{L}_a^D = \mathbb{E}_{x \sim p_{\text{data}(x)}, \mathbf{v} \sim p_{\text{attr}}} \log D(G_{\text{dec}}(G_{\text{enc}}^a(x, \mathbf{v}))) - \mathbb{E}_{y \sim p_{\text{data}(y)}} \log D(y). \quad (2)$$

In addition to the adversarial loss  $\mathcal{L}_a^G$ , we further use L1 distance to force the generator not only to generate realistic portraits to fool the discriminator but also get close to the human generated portrait. The L1 loss can be obtained as follows:

$$\mathcal{L}_{L1} = \mathbb{E}_{x, \mathbf{v}, y} \|y - G_{\text{dec}}(G_{\text{enc}}^a(x, \mathbf{v}))\|_1, \quad (3)$$

While the adversarial learning is employed on the system generated portrait  $\hat{y}$  to ensure its visual reality,  $\hat{y}$  is also expected to correctly contain the desired attributes  $\mathbf{v}$ . Hence, an attribute classifier  $F$  is used to constrain the system generated portrait  $\hat{y}$  with  $\mathbf{v}$ . Let  $\tilde{\mathbf{v}}$  denote the one-hot vectors of  $\mathbf{v}$ , the loss of the attribute classification  $L_c$  can be obtained as follows:

$$\mathcal{L}_c = \mathbb{E}_{x \sim p_{\text{data}(x)}, \mathbf{v} \sim p_{\text{attr}}} [\rho(F(G_{\text{dec}}(G_{\text{enc}}^a(x, \mathbf{v}))), \tilde{\mathbf{v}})], \quad (4)$$

where  $\rho$  is the summation of binary cross-entropy losses of all attributes as follows:

$$\rho(\hat{\mathbf{v}}, \tilde{\mathbf{v}}) = \sum_{i=1}^n -\tilde{v}_i \log \hat{v}_i - (1 - \tilde{v}_i) \log(1 - \hat{v}_i). \quad (5)$$

where  $\hat{v}_i = F_i(G_{\text{dec}}(G_{\text{enc}}^a(x, \mathbf{v})))$  indicates the prediction of the  $i^{\text{th}}$  attribute  $\mathbf{v}_i$ .

Overall, by combining the adversarial loss and the attribute classification loss, the final objective functions of the generator  $G$  and the discriminator  $D$  are as follows:

$$\mathcal{L}^G = \mathcal{L}_a^G + \lambda_1 \mathcal{L}_c + \lambda_2 \mathcal{L}_{L1}. \quad (6)$$

$$\mathcal{L}^D = \mathcal{L}_a^D + \lambda_3 \mathcal{L}_c. \quad (7)$$

where  $\lambda_1, \lambda_2, \lambda_3$  are hyper-parameters that control the relative importance of the losses.

## 2.4. Training and Testing Process

In the training phase, we use photo-attribute-portrait training samples  $\{(x^{(i)}, \mathbf{v}^{(i)}, y^{(i)})\}_{i=1}^N$  to train our model.

The generator  $G$  takes  $x$  and  $\mathbf{v}$  as input and generate the portraits  $\hat{y}$ . The discriminator  $D$  learns to distinguish real and generated samples by taking the generated portraits from  $G$  and the human generated portraits  $y$ , respectively. In the testing phase, the photo-attribute pairs are fed into  $G$  to generate portraits  $\hat{y}$ .

## 3. Experiments

### 3.1. Data and Experiment Setting

**Datasets.** One major challenge for this task lies in the lack of training data. During COVID-19 quarantine, art museums have challenged art lovers to recreate their favorite masterpieces and post photos of themselves. We have collected 4,608 such photo-portrait pairs from various sources including: (1) the museum artwork remake challenges that requires people to re-create artworks at home (e.g., the Getty Museum Challenge [15], Metropolitan Museum [16], Pinchuk Art Centre [17], and Rijksmuseum [18]); (2) Tussen Kunst & Quarantaine Instagram [19] that shares homemade recreations, (3) a remake project [20] built by Booooooom & Adobe to remake a famous work of art using photography; and (4) the remake images collected by Pinterest [21]. We manually remove non-human and bad quality photo-portrait pairs, and remove duplicated portraits. We use the Amazon Sandbox platform to perform dual attribute annotations and careful adjudication on the portraits. 3,296 high resolution pairs are selected and cropped to include only the face region. We use 3,098 pairs for training and 198 pairs for testing.

In addition, we have collected 51,939 portraits from Wikiart [22] (25,588 portraits) and Wikidata [23] (26,351 portraits) without attribute annotations, and included them in our released benchmark, for future work on learning visual features for various genres and potentially with less human supervision.

**Baselines.** The first baseline is a simple implementation of an image-to-image style transfer model. The input photos are transferred into portrait style by using a UNet-based generator and a discriminator is used to play against the generator. We also compare with two state-of-the-art image generation methods, StarGAN [24] and AttGAN [9].

**Experiment Setting.** In our experiments, we set the epoch number to 600 and the batch size to 32. The images are augmented by rotating, normalizing, and flipping before training to encourage the generalization of the model. The learning rate is 0.0002 and the Adam optimizer ( $\beta_1 = 0.5, \beta_2 = 0.999$ ) is used. The slope of leaky ReLU is 0.2 and dropout rate is 0.5.

### 3.2. General Generation Quality

A good portrait must attract our eyes in some way: its subject matter, it's use of color, an interesting juxtaposition

Method	IS $\uparrow$	FID $\downarrow$
Baseline	$1.68 \pm 0.148$	0.063
<i>MUSE</i> (ours)	<b><math>1.78 \pm 0.182</math></b>	<b>0.056</b>

Table 3. Quantitative comparison between the baseline and proposed *MUSE* on proposed portrait dataset.

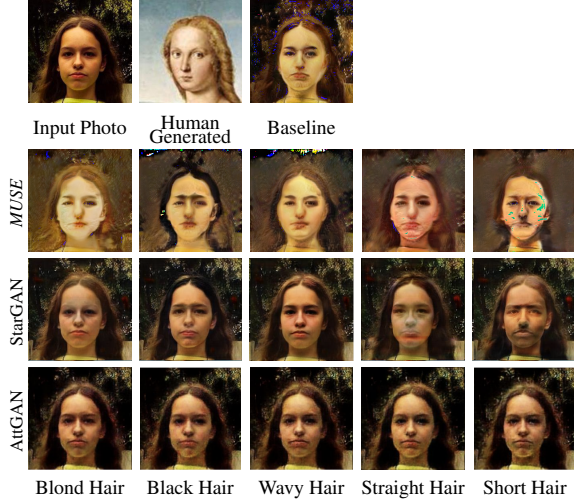


Figure 3. Synthetic portraits of the proposed *MUSE*, StarGAN [24] and AttGAN [9] trained on the portrait dataset given hair color.

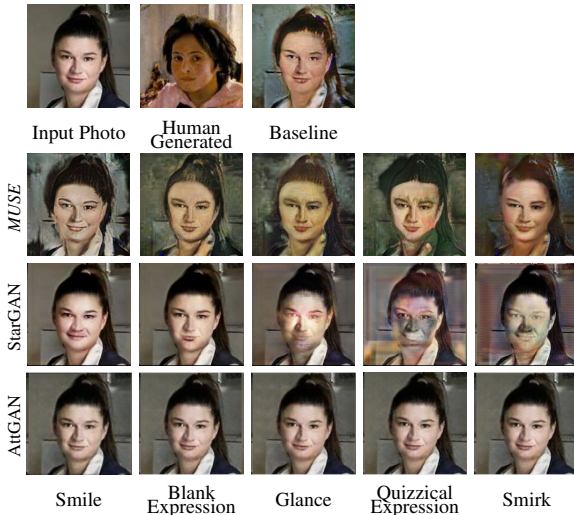


Figure 4. Synthetic portraits of the proposed *MUSE*, StarGAN [24] and AttGAN [9] trained on our portrait dataset given an attribute of face expression.

of objects, its realistic appearance, or any number of other factors. We evaluate the general visual quality of a portrait using the standard metric Inception Score (IS) [11] based on ImageNet [25] predefined classes. Suppose  $\mathcal{V}_g$  is the collection of generated portraits from the last layer of the generator  $G_M$  from the generation stack. We feed all generated portraits  $v \in \mathcal{V}_g$  into Inceptiv-v3 networks [26] to obtain their conditional probability distributions  $p(s|v)$  over 1000 ImageNet [25] classes, where each class is denoted by  $s$ . Class distribution is then marginalized by assuming uni-

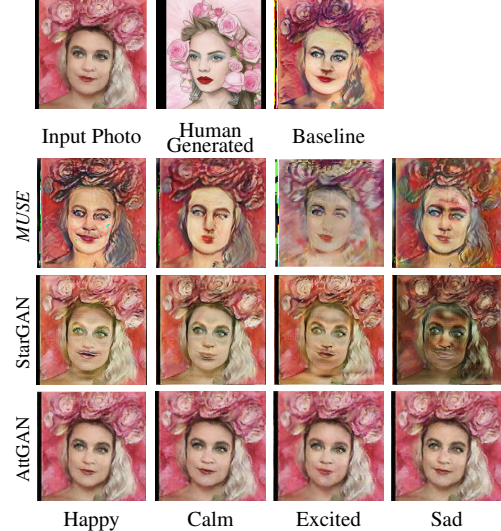


Figure 5. Synthetic portraits of the proposed *MUSE*, StarGAN [24] and AttGAN [9] trained on our portrait dataset given an attribute of mood expression.

form distribution of  $v \in \mathcal{V}_g$ , i.e.

$$q(s) = \sum_{v \in \mathcal{V}_g} p(s|v) \frac{1}{|\mathcal{V}_g|}.$$

IS score is the average KL-divergence between  $p_v = p(\cdot|v)$  and marginal distribution  $q(\cdot)$ ,

$$\text{IS}(\mathcal{V}_g) = \frac{1}{|\mathcal{V}_g|} \sum_{v \in \mathcal{V}_g} D_{\text{KL}}(p_v \| q),$$

A higher IS indicates the generated images are more realistic in the sense that their conditional distributions concentrate on a small subset of classes. Although IS is widely used, it does not compare the generated results with real samples [27]. Fréchet Inception Distance (FID) [27] is another popular metric for conditioned image generation, which measures the Fréchet distance between the generated image distribution and the real image (gold standard) distribution. Lower FID is better, indicating the generated results and target samples are more similar.

As shown in Table 3, the proposed *MUSE* outperforms the baseline with the IS score increased by 6% and the FID score decreased by 11%, respectively. By taking attribute embeddings as additional input, the model can build the alignment between the input photo and target portrait more easily, making the hidden representation more meaningful to produce more reasonable composition. For example, the attribute value `blond hair` can provide clearer guidance of generating a particular hair color rather than some unpredictable behavior.

### 3.3. Illustrating Textual Attributes

We propose a new metric to check if the generated portraits reflect the input attribute values, and further explore

Evaluation Method	Age	Clothing	Face	Gender	Hair	Mood	Pose	Setting	Style	Time	Weather	Average
Computer	0.88	0.78	0.82	0.99	0.86	0.72	0.59	0.54	0.95	0.56	0.83	0.78
Random	0.20	0.07	0.07	0.33	0.17	0.14	0.10	0.10	0.13	0.33	0.10	0.16

Table 4. Attribute reconstruction accuracy by calculating the F-score of the attributes of the system generated portrait and the ground-truth attributes from the human generated portraits.

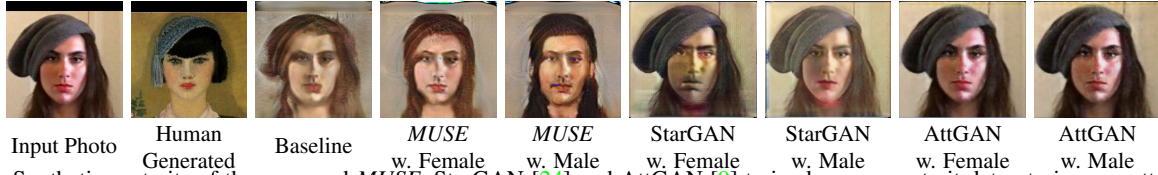


Figure 6. Synthetic portraits of the proposed *MUSE*, StarGAN [24] and AttGAN [9] trained on our portrait dataset given an attribute of gender.

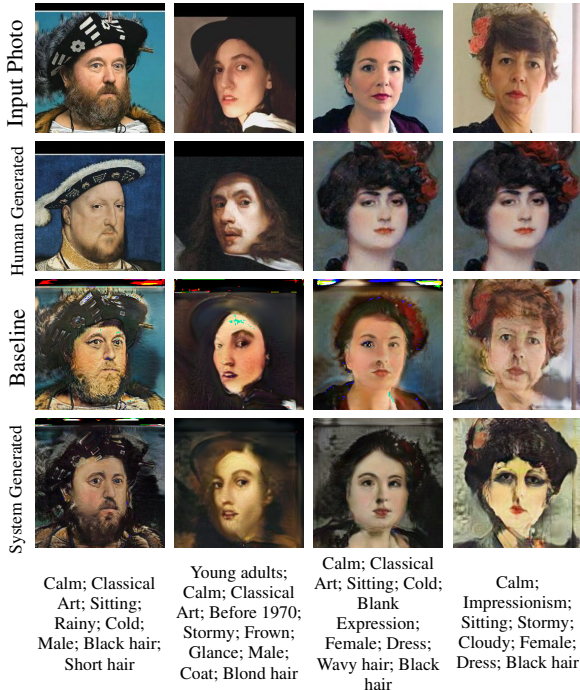


Figure 7. Synthetic portraits of the proposed *MUSE* trained on our portrait dataset given combined attributes including age, mood, style, time, pose, setting, weather, face expression, gender, clothing and hair.

how attribute semantics are learned and grounded into generated portraits.

**Subject Attribute Reconstruction Accuracy.** Since most of ImageNet classes are objects and the number of classes that appear in portraits is quite limited, the IS metric cannot evaluate the subtle details of human subjects in portraits. We use our attribute classifier  $F$  trained on the portrait data set to classify each generated portrait. We compute the F-score of the estimated attributes against the textual attributes extracted from the human generated portrait. Table 4 shows the attribute reconstruction accuracy. We can see that our approach successfully illustrates 78% attributes.

**Single Attribute Coherence** We first consider a simpler

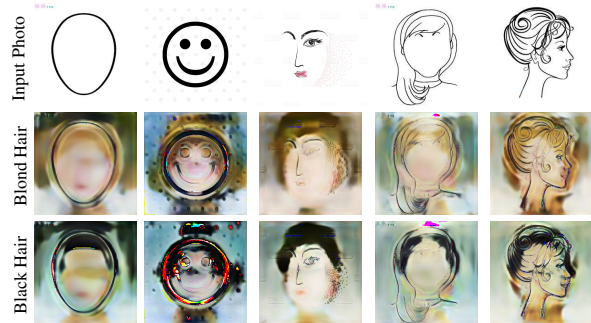


Figure 8. Given drawn sketches and an attribute of hair color or weather, the attribute value can be correctly grounded in the generated portraits.

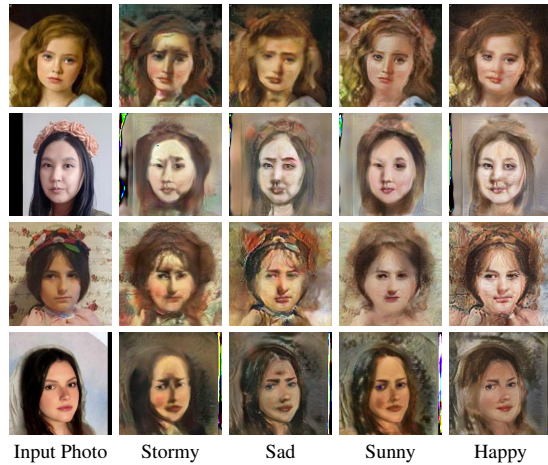


Figure 9. Inter-dependency of attributes.

scenario where we consider changing only one attribute. We train a separate model for each attribute, for which we constrain the attribute embeddings  $\mathbf{v}$  to contain only the specific attribute (e.g. `hair`) during training. Figures 3 to 6 show example outputs of the proposed *MUSE* compared with StarGAN [24] and AttGAN [9] by modifying hair, face expression, mood and gender respectively. We can see our models have successfully changed these attributes and learned to generate according to attribute values rather than performing some random behav-

ior. On the contrary, the StarGAN mistakenly interprets the attributes and AttGAN does not learn from the attributes at all, due to the small amount of training data and lacking of the mechanisms for cross-domain (photo to portrait) image transformation.

**Multiple Attributes** Here we consider a more complex scenario that we change all attributes for portrait generation. Figure 7 shows examples using a combination of 11 attributes listed in Table 2. We can see *MUSE* can capture the explicit attribute values such as `blond` and `black` hair, and capture the abstract concepts such as `stormy` vs `sunny` and `cold` vs `hot` by adjusting the background darkness levels.

**Grounding of Attributes** We further examine how the model ground attributes into generated portraits, by taking an demonstrative example of the `hair` attribute as shown in Figure 8. From these results we observe that *MUSE* can rely on either face outlines or facial features such as eyes or mouths to estimate the relative position of components including hair and facial area. In the fourth column we design a blank face with hair outline. Although *MUSE* cannot perfectly color the hair area, we do observe the model tends to color along the lines. We also show in the last column that *MUSE* works in a similar way for faces in profile.

**Inter-dependency of Attributes** As discussed in section 2.1, the attribute values in Table 2 are correlated. Here we show some examples of two related attributes, `weather` and `mood`, in Figure 9. For example, the `happy` portrait in the same row is associated with a brighter background implying a sunny weather. We also use the pre-trained classifier  $F$  to quantitatively evaluate the inter-dependency between `weather` and `mood`. Given the `happy` portraits, the predicted probabilities to be `sunny` and `stormy` are 38.28% and 0.22%, respectively. Similarly, given the `sunny` portraits, the predicted probabilities to be `happy` and `sad` are 39.20% and 0.31%, respectively.

**Affordances of Attributes** Not all the compositions of attributes are semantically valid. For example, it is not possible to have “smile” face expression and “sad” mood in the same portrait. Although it is challenging to inform a model with such affordances, we can use visual signal to improve the generalization capabilities of the model since invalid combinations will not appear in visual domain. Table 5 shows the attribute reconstruction accuracy, IS score and the FID score of the generated “smile sad” and “smile happy” portraits. Using a valid attributes combination, the model can generate a portrait with better quality and better reconstruction accuracy.

### 3.4. Remaining Challenges

Good art works should reflect not only explicit information of the subject but also implicit attributes such as personality, occasion, occupation, nationality, hobby. How-

Attributes	Recons. Acc. ↑		IS ↑	FID ↓
	Mood	Face		
Smile+Sad	0.960	0.934	$1.76 \pm 0.193$	0.085
Smile+Happy	<b>1.000</b>	<b>0.969</b>	<b><math>1.84 \pm 0.212</math></b>	<b>0.073</b>

Table 5. Attributes affordances of the proposed *MUSE* evaluated on various combination of mood and face expression.

ever, the portrait attribute types in the proposed data set are limited due to the lack of knowledge of the subject and the artist. Automatically extracting the implicit information from professionally written text descriptions of the portraits can enrich the attribute types and further enrich the generated portraits. In addition, instead of generating only face regions, artists often include more complete portrait paintings containing background landscape, pose & gestures and other objects. However, with the small amount of training samples, it is difficult to simultaneously handle all styles and content with large variation.

## 4. Related Work

Generative Adversarial Networks (GAN) [14] achieve great success in generating realistic images without much control [28]. Image-to-image generation [29, 3] takes an image as input condition, and transfers it into another image in a different domain, including satellite-to-map generation, sketches-to-shoes generation, night-to-day generation and Landscape-to-Photo generation.

Another line of work takes natural language as input condition and generates images accordingly. [30] first introduces a conditional DC-GAN architecture which achieves positive results for generating low-resolution images ( $64 \times 64$ ), but it is not equally successful in higher resolution image generation. To address this problem, Zhang *et al.* [31] propose Stacked Generative Adversarial Networks (StackGAN) that first generate low resolution images and make refinements thereafter. [32] further proposes hierarchically-nested losses that refines images in multiple steps. [33] uses dual inference over conditional and unconditional latent variables for disentanglement of content and style. Rather than starting from low-resolution image generation, [34] first constructs semantic layouts from text and generates images based on them. Despite promising results, the above methods only incorporate sentence-level features without considering fine-grained attributes and thus yield unsatisfactory results when the input sentences are complex.

Xu *et al.* [35] proposes Attentional GAN (AttnGAN) to enable the generative networks to be trained on words of higher relevance, and develops an *inter-modal* attention mechanism to compute the similarity between the generated image and the relevant text description. Recent methods [36, 37] incorporate attention mechanism to improve semantic consistency. They rely on general caption-type instructions to generate images of flowers[38], birds[39] or

common objects[40]. However, such instructions usually lack of identity information, which makes these models impossible to generate images of a specific person, flower or bird. In contrast, we propose to take both photo and textual attributes as input. It is worth noting that although AttGAN also leverages facial attributes when generating images, our model is different from the following aspects: 1) our goal is to generate creative and abstract portraits instead of generating photo-realistic images. 2) we apply more complex and abstract attributes to guide the portrait generation. For each attribute type, we include more values and some of them have shared semantics. Also our attributes are carefully designed for portraits and are more abstract such as mood and weather. In addition, we use trainable attribute embeddings to better represent the inter-dependency between multiple attribute values.

[41] describes an interesting user study to evaluate the results of generating animations from screenplays where users are asked to evaluate, on a five-point Likert scale [42], if the video shown was a reasonable animation for the text, how much of the text information was depicted in the video and how much of the information in the video was present in the text. Our attribute reconstruction metric aims at a similar goal, but we compute the scores based on pre-defined attribute categories and thus our metric is more objective.

## 5. Conclusions and Future Work

We have developed a novel method, *MUSE*, which can precisely illustrate textual attributes using portrait generation. In the future we plan to extend *MUSE* to unstructured text descriptions and apply open-domain attribute extraction techniques to extract as input, and extend it to cover a wider range of entity types and attribute types.

## References

- [1] Jeffrey Pennington, Richard Socher, and Christopher D. Manning. Glove: Global vectors for word representation. In *Empirical Methods in Natural Language Processing (EMNLP)*, pages 1532–1543, 2014. 1, 2
- [2] Jing Liao, Yuan Yao, Lu Yuan, Gang Hua, and Sing Bing Kang. Visual attribute transfer through deep image analogy. *ACM Transactions on Graphics*, 36(4), 2017. 1
- [3] Jun-Yan Zhu, Taesung Park, Phillip Isola, and Alexei A. Efros. Unpaired image-to-image translation using cycle-consistent adversarial networks. In *Proceedings of the IEEE International Conference on Computer Vision*, 2017. 1, 7
- [4] Jun-Yan Zhu, Richard Zhang, Deepak Pathak, Trevor Darrell, Alexei A Efros, Oliver Wang, and Eli Shechtman. Toward multimodal image-to-image translation. In *Proceedings of the 2017 Advances in Neural Information Processing Systems*. 2017. 1
- [5] Hsin-Ying Lee, Hung-Yu Tseng, Jia-Bin Huang, Maneesh Kumar Singh, and Ming-Hsuan Yang. Diverse image-to-image translation via disentangled representations. In *Proceedings of the 15th European Conference on Computer Vision*, September 2018. 1
- [6] T. Qiao, W. Zhang, M. Zhang, Z. Ma, and D. Xu. Ancient painting to natural image: A new solution for painting processing. In *2019 IEEE Winter Conference on Applications of Computer Vision (WACV)*, pages 521–530, 2019. 1
- [7] Gordon C. Aymar. The art of portrait painting. *Chilton Book Co., Philadelphia*, p. 119, 1967. 1
- [8] Olaf Ronneberger, Philipp Fischer, and Thomas Brox. U-net: Convolutional networks for biomedical image segmentation. In Nassir Navab, Joachim Hornegger, William M. Wells, and Alejandro F. Frangi, editors, *Medical Image Computing and Computer-Assisted Intervention – MICCAI 2015*, pages 234–241, Cham, 2015. Springer International Publishing. 2, 3
- [9] Zhenliang He, Wangmeng Zuo, Meina Kan, Shiguang Shan, and Xilin Chen. AttGAN: Facial attribute editing by only changing what you want. *IEEE Transactions on Image Processing*, 28(11):5464–5478, 2019. 2, 4, 5, 6
- [10] Xiaodan Hu, Mohamed A. Naiel, Alexander Wong, Mark Lamm, and Paul Fieguth. Runet: A robust unet architecture for image super-resolution. In *2019 IEEE/CVF Conference on Computer Vision and Pattern Recognition Workshops (CVPRW)*, pages 505–507, 2019. 2, 3
- [11] Tim Salimans, Ian J. Goodfellow, Wojciech Zaremba, Vicki Cheung, Alec Radford, and Xi Chen. Improved techniques for training GANs. *CoRR*, abs/1606.03498, 2016. 2, 5
- [12] Tomas Mikolov, Kai Chen, Greg Corrado, and Jeff Dean. Efficient estimation of word representations in vector space. In Yoshua Bengio and Yann LeCun, editors, *1st International Conference on Learning Representations, ICLR 2013, Scottsdale, Arizona, USA, May 2-4, 2013, Workshop Track Proceedings*, 2013. 3
- [13] Vinod Nair and Geoffrey E. Hinton. Rectified linear units improve restricted boltzmann machines. In *Proceedings of the 27th International Conference on International Conference on Machine Learning*, 2010. 3
- [14] Ian Goodfellow, Jean Pouget-Abadie, Mehdi Mirza, Bing Xu, David Warde-Farley, Sherjil Ozair, Aaron Courville, and Yoshua Bengio. Generative adversarial nets. In *Proceedings of the 28th Annual Conference on Neural Information Processing Systems*. 2014. 4, 7
- [15] Getty Museum. <https://twitter.com/GettyMuseum>. [Online]. 4
- [16] Mett Winning. <https://www.instagram.com/explore/tags/mettwinning/>. [Online]. 4
- [17] Pinchuk Art Centre. <http://new.pinchukartcentre.org/>. [Online]. 4
- [18] Rijksmuseum. <https://www.rijksmuseum.nl/en>. [Online]. 4
- [19] Tussen Kunst & Quarantaine. <https://www.instagram.com/tussenkunstenquarantaine/>. [Online]. 4

- [20] Booooooom. <https://www.booooooom.com/2011/09/27/remake-a-project-by-booooooom-and-adobe/>. [Online]. 4
- [21] Pinterest. <https://www.pinterest.com/>. [Online]. 4
- [22] Wikiart. <https://www.wikiart.org/>. [Online]. 4
- [23] Wikidata. <https://www.wikidata.org/>. [Online]. 4
- [24] Yunjei Choi, Min-Je Choi, Munyoung Kim, Jung-Woo Ha, Sunghun Kim, and Jaegul Choo. Stargan: Unified generative adversarial networks for multi-domain image-to-image translation. *CoRR*, 2017. 4, 5, 6
- [25] J. Deng, W. Dong, R. Socher, L. Li, Kai Li, and Li Fei-Fei. ImageNet: A Large-Scale Hierarchical Image Database. In *Proceedings of the IEEE International Conference on Computer Vision*, 2009. 5
- [26] Christian Szegedy, Vincent Vanhoucke, Sergey Ioffe, Jonathon Shlens, and Zbigniew Wojna. Rethinking the inception architecture for computer vision. *CoRR*, abs/1512.00567, 2015. 5
- [27] Martin Heusel, Hubert Ramsauer, Thomas Unterthiner, Bernhard Nessler, Günter Klambauer, and Sepp Hochreiter. GANs trained by a two time-scale update rule converge to a nash equilibrium. *CoRR*, abs/1706.08500, 2017. 5
- [28] Mehdi Mirza and Simon Osindero. Conditional generative adversarial nets. *CoRR*, abs/1411.1784, 2014. 7
- [29] Phillip Isola, Jun-Yan Zhu, Tinghui Zhou, and Alexei A. Efros. Image-to-image translation with conditional adversarial networks. In *Proceedings of the IEEE Computer Society Conference on Computer Vision and Pattern Recognition*, 2017. 7
- [30] Scott E. Reed, Zeynep Akata, Xinchun Yan, Lajanugen Logeswaran, Bernt Schiele, and Honglak Lee. Generative adversarial text to image synthesis. In *Proceedings of the 33rd International Conference on International Conference on Machine Learning*, 2016. 7
- [31] Han Zhang, Tao Xu, Hongsheng Li, Shaoting Zhang, XiaoLei Huang, Xiaogang Wang, and Dimitris N. Metaxas. StackGAN: Text to photo-realistic image synthesis with stacked generative adversarial networks. In *Proceedings of the IEEE International Conference on Computer Vision*, 2017. 7
- [32] Zizhao Zhang, Yuanpu Xie, and Lin Yang. Photographic text-to-image synthesis with a hierarchically-nested adversarial network. In *Proceedings of the IEEE Computer Society Conference on Computer Vision and Pattern Recognition*, pages 6199–6208, 2018. 7
- [33] Qicheng Lao, Mohammad Havaei, Ahmad Pesaraghader, Francis Dutil, Lisa Di-Jorio, and Thomas Fevens. Dual adversarial inference for text-to-image synthesis. In *2019 IEEE/CVF International Conference on Computer Vision, ICCV 2019, Seoul, Korea (South), October 27 - November 2, 2019*, pages 7566–7575. IEEE, 2019. 7
- [34] Seunghoon Hong, Dingdong Yang, Jongwook Choi, and Honglak Lee. Inferring semantic layout for hierarchical text-to-image synthesis. In *Proceedings of the IEEE Computer Society Conference on Computer Vision and Pattern Recognition*, pages 7986–7994, 2018. 7
- [35] Tao Xu, Pengchuan Zhang, Qiuyuan Huang, Han Zhang, Zhe Gan, Xiaolei Huang, and Xiaodong He. AttnGAN: Fine-grained text to image generation with attentional generative adversarial networks. *CoRR*, abs/1711.10485, 2017. 7
- [36] Tingting Qiao, Jing Zhang, Duanqing Xu, and Dacheng Tao. Mirrorgan: Learning text-to-image generation by redescription. In *Proceedings of the IEEE Computer Society Conference on Computer Vision and Pattern Recognition*, 2019. 7
- [37] Hongchen Tan, Xiuping Liu, Xin Li, Yi Zhang, and Baocai Yin. Semantics-enhanced adversarial nets for text-to-image synthesis. In *Proceedings of the IEEE International Conference on Computer Vision*, pages 10500–10509, 2019. 7
- [38] Maria-Elena Nilsback and Andrew Zisserman. Automated flower classification over a large number of classes. In *Sixth Indian Conference on Computer Vision, Graphics & Image Processing, ICVGIP 2008, Bhubaneswar, India, 16-19 December 2008*, pages 722–729. IEEE Computer Society, 2008. 7
- [39] Catherine Wah, Steve Branson, Peter Welinder, Pietro Perona, and Serge Belongie. The caltech-ucsd birds-200-2011 dataset. 2011. 7
- [40] Tsung-Yi Lin, Michael Maire, Serge J. Belongie, James Hays, Pietro Perona, Deva Ramanan, Piotr Dollár, and C. Lawrence Zitnick. Microsoft COCO: common objects in context. In David J. Fleet, Tomás Pajdla, Bernt Schiele, and Tinne Tuytelaars, editors, *Computer Vision - ECCV 2014 - 13th European Conference, Zurich, Switzerland, September 6-12, 2014, Proceedings, Part V*, volume 8693 of *Lecture Notes in Computer Science*, pages 740–755. Springer, 2014. 8
- [41] Yeyao Zhang, Eleftheria Tsipidi, Sasha Schriber, Mubbasir Kapadia, Markus Gross, and Ashutosh Modi. Generating animations from screenplays. In *Proceedings of the Eighth Joint Conference on Lexical and Computational Semantics*, 2019. 8
- [42] Rensis Likert. A technique for the measurement of attitudes. *Archives of Psychology*, 22(140):1–55, 1932. 8